Electronic Supplementary Material (ESI) for Physical Chemistry Chemical Physics.

Supplementary Information to "Tuning switching behavior of binary oxides-based resistive memories by inserting an ultra-thin chemically active metal nanolayer: a case study on Ta_2O_5-Ta system"

Shuang Gao, Fei Zeng,[a)]* Minjuan Wang, Guangyue Wang, Cheng Song and Feng Pan[b)]*

Laboratory of Advanced Materials (MOE), School of Materials Science and Engineering,

Tsinghua University, Beijing 100084, People's Republic of China

[a)]E-mail: zengfei@mail.tsinghua.edu.cn. Tel.: +86-10-62795373

[b)]E-mail: panf@mail.tsinghua.edu.cn. Tel.: +86-10-62772907

SI1. The endurance, uniformity, and retention characteristics of the nonpolar switching behavior in Pt/Ta_2O_5(10 nm)/Pt device, self-compliance bipolar switching behavior in Pt/Ta_2O_5(4 nm)/Ta(2 nm)/Ta_2O_5(4 nm)/Pt device, and CRS behavior in Pt/Ta_2O_5(3 nm)/Ta(4 nm)/Ta_2O_5(3 nm)/Pt device.

The endurance, uniformity, and retention characteristics of the devices are provided in Fig. SI1. By comparing the results in Figs. SI1a, SI1e, and SI1i, one can obtain that, under successive DC switching operation, the endurance characteristics of Pt/Ta_2O_5(4 nm)/Ta(2 nm)/Ta_2O_5(4 nm)/Pt and Pt/Ta_2O_5(3 nm)/Ta(4 nm)/Ta_2O_5(3 nm)/Pt devices are less satisfactory than that of Pt/Ta_2O_5(10 nm)/Pt device. However, it is noted that the endurance failures in Figs. SI1e and SI1i are believed to be caused by voltage overstress and are expected to be significantly alleviated by using the operation method proposed in Ref. S1. The uniformity characteristics are revealed by examining the evolutions of critical switching parameters, including resistances and threshold voltages, during successive DC switching operation, as shown in Figs. SI1b, SI1c, SI1f, SI1g, SI1j, and SI1k. One can see from these figures that except the R_{HRS}@-0.1 V and V_{set} of Pt/Ta_2O_5(10 nm)/Pt device, all other switching parameters exhibit acceptable uniformity. The retention characteristics are evaluated by examining the evolutions of resistances with time under a constant voltage stress. The obtained results in Figs. SI1d, SI1h, and SI1l exhibit no degradation in resistances after a long period of 2 000 s, thus demonstrating satisfactory retention performance in all devices.

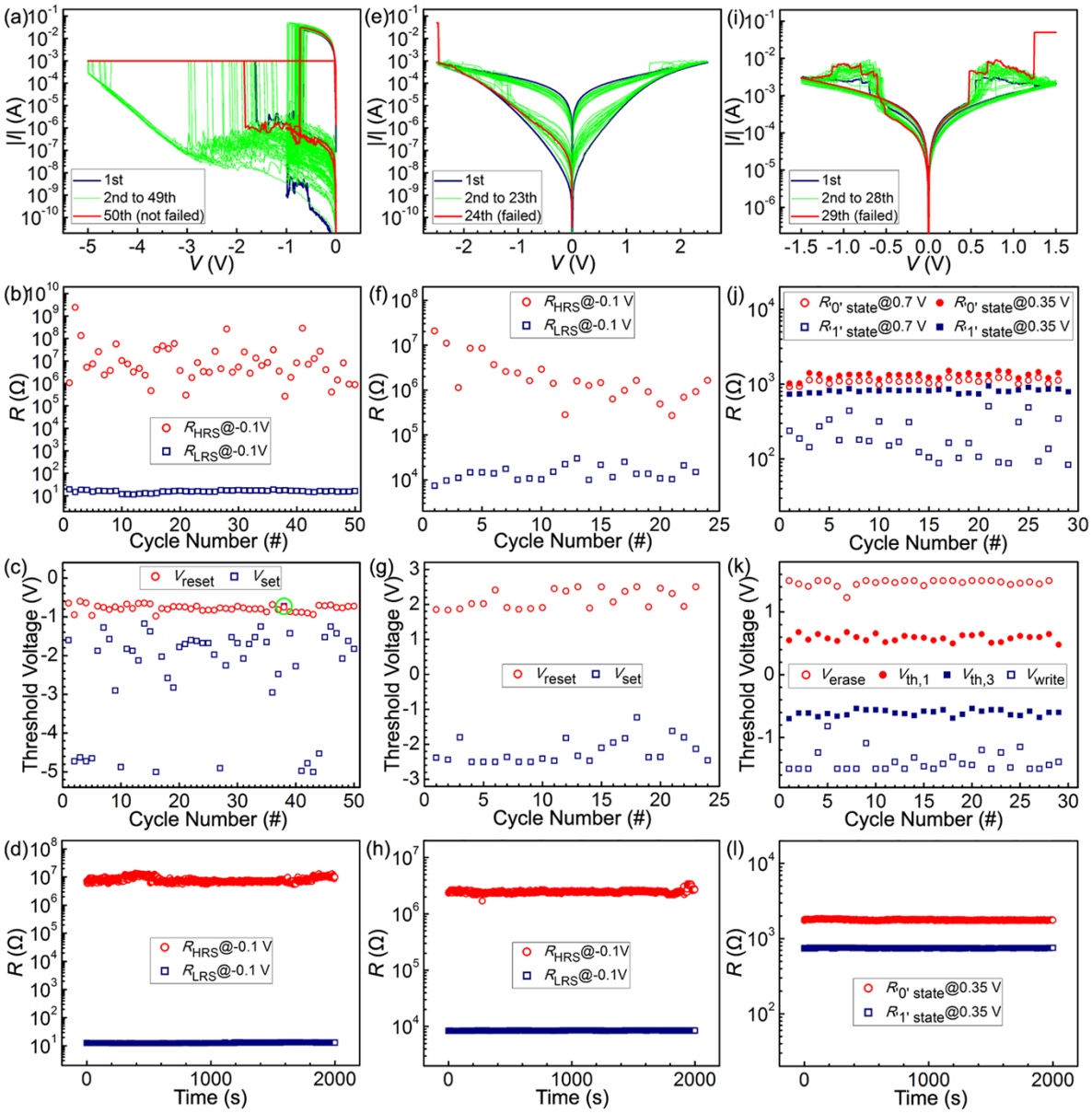

Fig. SI1 The endurance performance, evolution of resistances, evolution of threshold voltages, and retention performance of the (a–d) nonpolar switching behavior in Pt/Ta_2O_5(10 nm)/Pt device, (e–h) self-compliance bipolar switching behavior in Pt/Ta_2O_5(4 nm)/Ta(2 nm)/Ta_2O_5(4 nm)/Pt device, and (i–l) CRS behavior in Pt/Ta_2O_5(3 nm)/Ta(4 nm)/Ta_2O_5(3 nm)/Pt device. The green circle in (c) denotes the overlap between V_{set} and V_{reset}. The V_{erase}, $V_{th,1}$, $V_{th,3}$, and V_{write} are defined by referring to Ref. S2.

SI2. The analysis of conduction mechanisms for the LRS(nonpolar) and pristine state of the Pt/Ta_2O_5(4 nm)/Ta(2 nm)/Ta_2O_5(4 nm)/Pt device.

Fig. SI2a shows the *I*–*V* curve of the LRS(nonpolar) in a log-log coordinate. It is found that most of this curve can be well fitted by the ohmic conduction with $I \propto V$. The slight deviation at high voltage region is totally understandable and is due to the current-induced heating effect in a metallic filament.[S3] Hence this fitting result supports the formation of a metallic Ta filament in the LRS(nonpolar).

Fig. SI2b shows the I–$V^{0.5}$ curve of the pristine state in a semi-logarithmic coordinate. The good linear characteristic of this curve demonstrates that the pristine state follows the conduction mechanism of thermionic emission. This conduction mechanism suggests that there is no complete V_O or Ta filament in pristine state (sketch ① in Fig. 3c) and that the transport of electrons in pristine state under negative voltage polarity is limited principally by the emission of electrons from the Pt TE into the conduction band of the upper Ta_2O_5 layer.

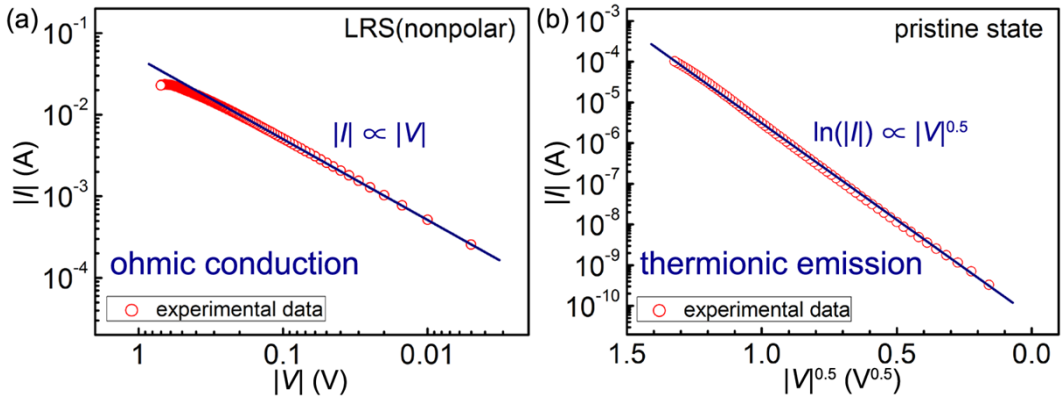

Fig. SI2 The analysis of conduction mechanisms for the (a) LRS(nonpolar) and (b) pristine state of the Pt/Ta_2O_5(4 nm)/Ta(2 nm)/Ta_2O_5(4 nm)/Pt device.

SI3. The device area-dependent self-compliance bipolar switching behaviors in Pt/Ta_2O_5(4 nm)/Ta(2 nm)/Ta_2O_5(4 nm)/Pt device

The navy *I–V* curve in Fig. SI3a is a duplication of the blue *I–V* curve in Fig. 3b in the main text, which was obtained with the Pt top electrode (~50 μm in diameter). Related LRS(bipolar) and HRS(bipoar) are denoted as LRS(bipolar,Pt) and HRS(bipoar,Pt), respectively. In contrast, the green *I–V* curve in Fig. SI3a was obtained by directly putting the inert tungsten probe (tip size: ~0.5 μm in radius of curvature) on the surface of the Ta_2O_5(4 nm)/Ta(2 nm)/Ta_2O_5(4 nm)/Pt structure. That is, the green *I–V* curve was obtained with the tungsten probe as top electrode. Related LRS(bipolar) and HRS(bipoar) are denoted as LRS(bipolar,probe) and HRS(bipoar,probe), respectively. For a rough estimation, the effective contact area with the tungsten probe as top electrode is assumed to be a circle with a diameter of ~1 μm. If so, the electrode area with the Pt top electrode is ~2 500 times of that with the tungsten probe as top electrode. Note that for a RRAM structure with a filamentary switching mechanism, the LRS resistance is almost independent of the device area, while the HRS resistance is almost inversely proportional to the device area.[S4,S5] This means that if the self-compliance bipolar switching behavior indeed originates from the formation and rupture of a V_O filament, one can expect that the LRS(bipolar,probe) resistance is almost equal to the LRS(bipolar,Pt) resistance, but the HRS(bipolar,probe) resistance is ~2 500 times of the HRS(bipolar,Pt) resistance. This expectation can be nicely met by the fact in Fig. SI3b that there is little difference between the LRS(bipolar,probe) resistance and the LRS(bipolar,Pt) resistance, while the HRS(bipolar,probe) resistance is ~600 times of the HRS(bipolar,Pt) resistance. Therefore, these results support the proposed filamentary switching model for the

self-compliance bipolar switching behavior of Pt/Ta_2O_5(4 nm)/Ta(2 nm)/Ta_2O_5(4 nm)/Pt device (Fig. 3c in the main text).

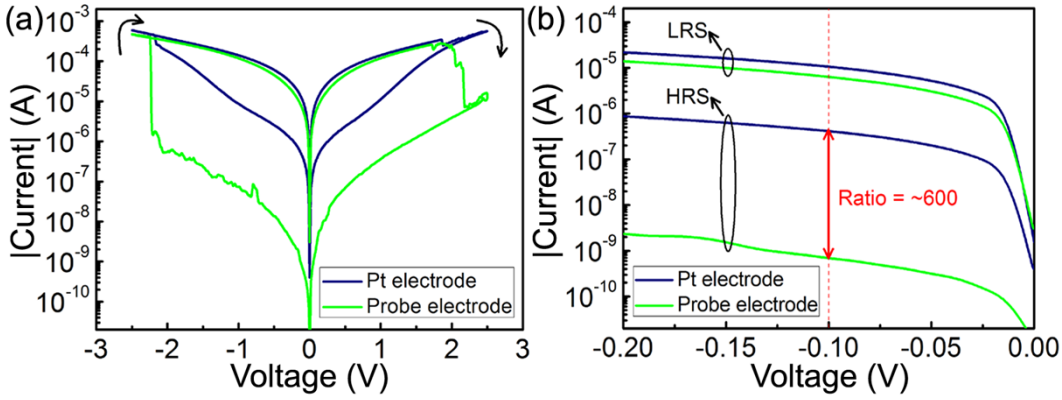

Fig. SI3 (a) The device area-dependent self-compliance bipolar switching behaviors in Pt/Ta_2O_5(4 nm)/Ta(2 nm)/Ta_2O_5(4 nm)/Pt device. (b) The enlarged view of (a) with a voltage region between –0.2 and 0 V.

SI4. The observation of CRS behavior after either +R or –R operation in the Pt/Ta_2O_5(3 nm)/Ta(4 nm)/Ta_2O_5(3 nm)/Pt device.

A CRS behavior can indeed be observed after either +R or –R operation in the Pt/Ta_2O_5(3 nm)/Ta(4 nm)/Ta_2O_5(3 nm)/Pt device, as demonstrated in Fig. SI4. Initially, the Pt/Ta_2O_5(3 nm)/Ta(4 nm)/Ta_2O_5(3 nm)/Pt device stays at the LRS(nonpolar) (sketch ③). A positive voltage sweep to 1.5 V can trigger the evolution of ③→⑤, as indicated by the black curve in Fig. SI4a. Subsequently, the evolutions of ⑤→⑥→④ and ④→⑥→⑤ occur during negative and positive voltage sweeps, respectively, resulting in the CRS behavior (the blue and red curves in Fig. SI4a). In contrast, the device in its initial LRS(nonpolar) can be reset into the HRS(nonpolar,–R) under a negative voltage sweep, i.e., the evolution of ③→④, as manifested by the black curve in Fig. SI4b. Subsequently, the evolutions of ④→⑥→⑤ and ⑤→⑥→④ appear during positive and negative voltage sweeps, respectively, leading to the CRS behavior (the blue and red curves in Fig. SI4b).

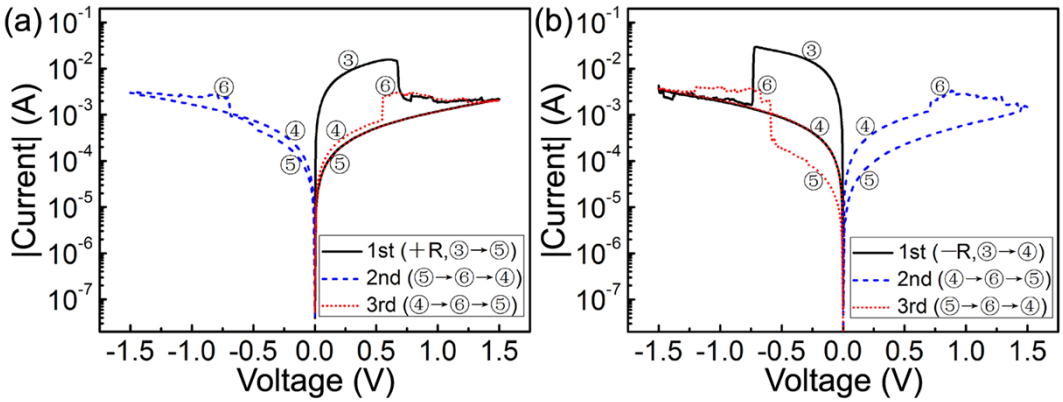

Fig. SI4 The CRS behaviors after (a) +R and (b) –R operations in the Pt/Ta_2O_5(3 nm)/Ta(4 nm)/Ta_2O_5(3 nm)/Pt device. The serial numbers in this figure have the same meaning as that in Fig. 5 in the main text.

SI5. The demonstration of hopping conduction in both '1' and '0' states of the Pt/Ta_2O_5(3 nm)/Ta(4 nm)/Ta_2O_5(3 nm)/Pt device.

Fig. SI5 shows the comparison between experimental data and fitting curves on the basis of hopping conduction for both '1' and '0' states of the Pt/Ta_2O_5(3 nm)/Ta(4 nm)/Ta_2O_5(3 nm)/Pt device. The good agreement between experimental data and fitting curves suggests the existence of a complete V_O filament in these two states, which is similar to that of the LRS(bipolar) of the Pt/Ta_2O_5(4 nm)/Ta(2 nm)/Ta_2O_5(4 nm)/Pt device. It has been acknowledged that, after the formation of a conducting filament, further modulation in its resistance is realized via electric field-induced lateral expansion/reduction.[S6] Hence, the evolution of ②↔⑦↔⑧ in Fig. 5 is believed to originate from the electric field-induced lateral expansion/reduction of V_O filaments in upper and lower Ta(4 nm)/Ta_2O_5(3 nm)/Pt devices.

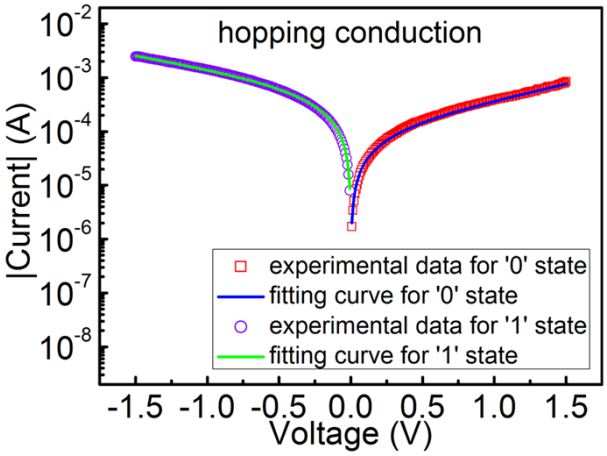

Fig. SI5 The comparison between experimental data and fitting curves on the basis of hopping conduction for both '1' and '0' states of the Pt/Ta_2O_5(3 nm)/Ta(4 nm)/Ta_2O_5(3 nm)/Pt device. fitting curve for '1' state, $|I| \propto [\exp(1.05 \cdot |V|) - \exp(-1.05 \cdot |V|)]$; fitting curve for '0' state, $I \propto [\exp(1.40 \cdot V) - \exp(-1.40 \cdot V)]$.

SI6. The discussion of ruling out other possible origins of the observed CRS behavior.

Since the 4 nm Ta nanolayer has been oxidized to some extent during the deposition of the upper Ta_2O_5 layer, it is acceptable to regard the upper Ta(4 nm)/Ta_2O_5(3 nm)/Pt device as a Ta/TaO_x(x<2.5)/Ta_2O_5/Pt device. If so, one may doubt whether the CRS behavior is contributed only by the Ta/TaO_x(x<2.5)/Ta_2O_5/Pt device, just as what is in Ref. S7. Besides, one may also doubt whether the CRS behavior is contributed only by the upper Ta(4 nm)/Ta_2O_5(3 nm)/Pt device with a similar switching mechanism to that in Ref. S8. In fact, these two possibilities can be easily and definitely ruled out based on the following reasons. First, as clearly written in Ref. S7, the realization of CRS behavior in a TaO_x/Ta_2O_5 bilayer structure requires a very precise control of V_O concentration in the TaO_x layer. It seems impossible that the TaO_x layer caused by Ta_2O_5 deposition can meet such a strict requirement. Second, in Ref. S8., the prerequisite for CRS behavior is the so-called soft reset process, which is not the case in the current work (see Figs. 5b and 5c). Third, in Refs. S7 and S8, the state obtained after forming process is the CRS 'ON' state. However, in the current work, the state obtained after forming process (i.e., the –HF process in Fig. 5b) is the CRS '1' state (see Figs. 5b and 5c), which is the feature of a standard CRS cell composed of two antiserial bipolar resistive memory cells.[S2] Taking these reasons into account, other possible origins of the CRS behavior in the current work can be ruled out undoubtedly.

References

S1 G. Wang, S. Long, Z. Yu, M. Zhang, T. Ye, Y. Li, D. Xu, H. Lv, Q. Liu, M. Wang, X. Xu, H. Liu, B. Yang, J. Suñé and M. Liu, *Appl. Phys. Lett.* 2015, **106**, 092103.

S2 E. Linn, R. Rosezin, C. Kügeler and R. Waser, *Nat. Mater.*, 2010, **9**, 403−406.

S3 U. Russo, D. Ielmini, C. Cagli, A. L. Lacaita, S. Spiga, C. Wiemer, M. Perego and M. Fanciulli, in *Proc. Int. Electron Devices Meet.*, Baltimore, MD, December 2007, 775–778.

S4 F. Pan, S. Gao, C. Chen, C. Song and F. Zeng, *Mater. Sci. Eng. R*, 2014, **83**, 1–59.

S5 R. Waser, R. Dittmann, G. Staikov and K. Szot, *Adv. Mater.*, 2009, **21**, 2632–2663.

S6 U. Russo, D. Kamalanathan, D. Ielmini, A. L. Lacaita and M. N. Kozicki, *IEEE Trans. Electron Dev.*, 2009, **56**, 1040–1047.

S7 Y. Yang, P. Sheridan and W. Lu, *Appl. Phys. Lett.*, 2012, **100**, 203112.

S8 G. Tang, F. Zeng, C. Chen, H. Liu, S. Gao, C. Song, Y. Lin, G. Chen and F. Pan, *Nanoscale*, 2013, **5**, 422–428.